

# Electrical charge measurements on ejecta from impact loading of explosive crystals

E. E. DONALDSON, M. H. MILES, J. T. DICKINSON

*Department of Physics, Washington State University, Pullman, Washington 99164-2814, USA*

Measurements of the properties of the small, macroscopic particles (ejecta) that are released from the impact loading of single crystals of pentaerythritol tetranitrate are presented. Total mass of the ejecta, total electrical charge on the ejecta, and approximate size distributions are also given. A few measurements were also performed on crystals of cyclotrimethylenetrinitramine and cyclotetramethylene tetranitramine.

## 1. Introduction

In a previous paper [1] we reported the production and properties of small macroscopic particles (ejecta) in the size range 0.1 to 500  $\mu\text{m}$  released from the fracture of solid materials. The materials studied included pure crystalline inorganic compounds, polymers and polymer matrix composites. Briefly, we observed that when materials were fractured in tension or in 3 point flexure loading:

1. The fracture of most solid materials produced ejecta.
2. In many cases the surface area of ejecta was appreciable and, in some cases, was greater than the cross-sectional area of the sample.
3. Ejecta tended to carry electrical charge. Individual ejecta particles were found to be charged either positively or negatively.
4. Ejecta were released with velocities as high as 50  $\text{m sec}^{-1}$ .

In this paper, we report the investigation of ejecta arising from the impact loading of crystalline pentaerythritol tetranitrate (PETN), cyclotrimethylenetrinitramine (RDX) and cyclotetra methylene tetranitramine (HMX). The choice of impact loading was made principally because of the small sample dimensions (typically, millimetre size crystals) and possible relevance to impact loading tests of explosive sensitivity [2, 3]. Earlier studies of PETN in our laboratory had demonstrated that impact crushing produced high levels of fracto emission [4] (defined as the emission of electrons, ions, neutral atoms and molecules, and photons due to deformation and fracture). Furthermore, long wavelength radiation (radiowave emission, RE) was detected during crushing and was attributed to small electrostatic discharges due to charge separation occurring across fracture surfaces. Our major goal in this study was to examine the possible electrical charge on the fragments produced by fracture. In addition, we measured the total yield and size distributions of the macroscopic particles created during impact loading which is used to estimate an average charge density on the ejecta surface.

## 2. Experimental details

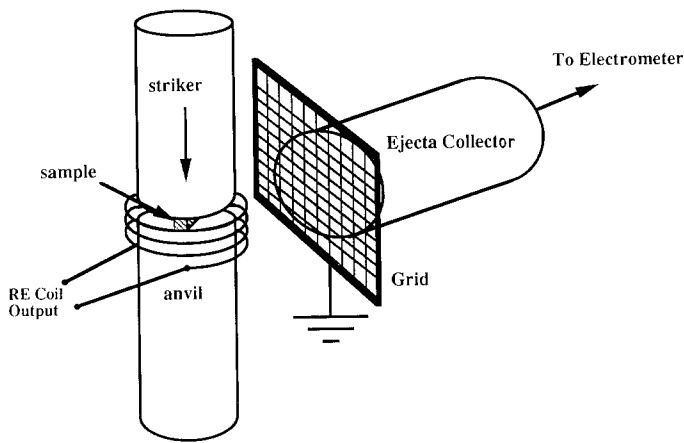
A sketch of the impact device used in these studies is shown in Fig. 1. The crystals were crushed between planar hardened steel surfaces, each 12 mm diameter. The striker was driven by a hammer blow to its top end providing an impulse of  $\sim 1 \text{ kg m sec}^{-1}$ . The time profile of the applied force was measured using a force transducer built into the anvil. When the hammer hit the striker, the force on the sample increased for approximately 100 to 200  $\mu\text{sec}$  then fell rapidly as the crystal collapsed. The maximum force was typically 5000 N.

The tests were conducted by placing a single crystal or several crystals of millimetre dimensions at the centre of the anvil and driving the striker down to impact them with a single blow. Under these experimental conditions, a single impact always crushed the crystals and produced ejecta without any evidence of ignition.

Subsequent impacts delivered to the sample after it had already been crushed usually caused ignition. The location of this ignition was usually near the edges of the crushing surfaces and produced ejecta in an obvious directional jet. Ignition always produced an accompanying plasma of highly charged species which we could not avoid collecting. To prevent this somewhat uncontrolled charge emission, we limited our measurements to single impact, purposefully avoiding ignition.

The mass of ejecta and their electrical charge was measured by catching the ejecta in a spun aluminium collector, 28 mm diameter, positioned as shown in Fig. 1. An electrically grounded metal screen was placed in front of the collector to shield it from any electrical activity in the fracture zone and also to prevent fragments larger than 1.5 mm from reaching the collector. Although the screen stopped some of the ejecta, it transmitted 60% of the smallest fragments. If the ejecta were to travel out in an axially symmetric distribution, then by geometry the screened collector should catch approximately 10% of all the ejecta released. In practice, the ejecta had a nonsymmetric

Figure 1 Sketch of the experimental configuration.



randomly oriented distribution, even when ignition was avoided. However, by repeating experiments we were able to obtain average characteristics of the ejecta.

For charge measurements, the aluminium collector was connected by a short coaxial cable to a coulombmeter. As charged ejecta were captured by the collector, an equal charge would flow to the coulombmeter. After the total collected charge was determined, the ejecta were transferred to a small piece of thin aluminium foil for weighing with a Cahn Model No. 21 Automatic Electrobalance. Most of the results reported here are on PETN because of availability of sample material. A few measurements were also performed on crystals of RDX and HMX.

### 3. Results and discussion

#### 3.1. Total mass

In the case of PETN, the total mass of ejecta collected from impact was on average 1.3% of the mass of the original PETN crystal samples. The samples were pulverized, with the greater part of each sample remaining attached to the metal impacting surfaces. As might be expected, the ejecta produced by impact formed a larger fraction of the total mass than the ejecta from materials examined in tensile or flexure loading [1]. The large amount of ejecta was collected because the entire sample was pulverized, the efficient transfer of vertical momentum to horizontal momentum through compressive shear deformation, and because of channelling by the impacting surfaces in a planar distribution. Similar effects were obtained for RDX and HMX crystals.

#### 3.2. Trajectories

We found that a large fraction of the ejecta reached the far end of our ejecta collector, that is, they were able to travel at least 6 cm from the crushing region. Measurements described later indicate that the most probable ejecta size is about  $5 \mu\text{m}$ . Calculations based on Stoke's law [5] show that  $5 \mu\text{m}$  spherical particles would travel horizontally less than 1 cm in still air even if they were launched with an initial speed of  $100 \text{ m sec}^{-1}$ . Lower initial speeds or irregularly shaped particles would result in a smaller range. Thus, we must conclude that a hydrodynamic effect is dominant, e.g. the burst of air created by rapid motion of the impacting surfaces carries entrained ejecta. This would imply that until turbulence set in, the particles

would move at approximately the speed of sound, followed by a rapid deceleration. A vacuum experiment is one possible means for obtaining more accurate initial velocities and trajectories.

#### 3.3. Electrical Charge

The PETN ejecta always carried a net negative charge. A comparison was made of the total mass of the collected PETN ejecta with the total charge carried by the ejecta for repeated experiments on specimens of similar size. Fig. 2 shows the resulting data and a least squares fit indicating that the total mass and total charge are positively correlated. We emphasize that these are total charge measurements and that the ejecta most likely contains charged patches of both signs, potentially involving considerably larger quantities of charge of each sign.

In contrast, the ejecta from crushing crystals of RDX displayed a much smaller charge per unit mass ( $1/20$  of that for PETN) and the charge measured was positive or negative. The charging of HMX ejecta was similar to that of RDX, namely the total charges/mass were an order of magnitude smaller than for PETN and were of either sign.

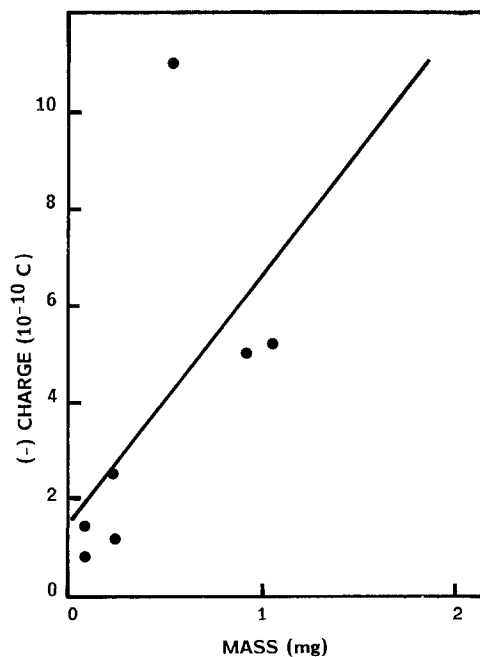


Figure 2 Graph of the electrostatic charge (negative) carried by the ejecta against mass of ejecta collected for PETN.

Because the ejecta were insulating particles, they lost little of their surface charge to the collector. Using this fact, we could test the conclusion that the majority of the charge we measured was indeed carried by the ejecta with the following procedure: after the charge of a sample of ejecta had been measured and recorded, the collector was electrically grounded. The ground on the collector was then removed and the ejecta were spilled out of the collector. The new value of charge registered during the removal of the ejecta was of opposite sign and nearly equal in magnitude to the charge originally collected. This result would not have occurred if a significant portion of the initial measured charge had been carried by electrons or ions emitted from the fracture zone, thus providing convincing evidence that the charge we measured was indeed carried by the ejecta particles.

### 3.4. Accompanying long wave length electromagnetic signals

In order to determine if electrostatic phenomena were accompanying the fracture event itself, we placed a flat coil having a diameter of 2 cm and inductance of  $\sim 10$  mH around the crushing region. Because the coil was sensitive to magnetic signals from the motion of steel components, we replaced the steel crusher with a brass-bronze impact device. The output of the coil was fed to a wide-band differential amplifier with a  $1\text{ M}\Omega$  input impedance, the output of which was digitized. When a rapid change in  $B$  field occurred, i.e. due to an electrostatic discharge, a ring-down burst of e.m.f. at a frequency of 200 kHz was produced. Because our coil was so close to the impact region, it was sensitive only to near-field components of the electromagnetic field. Tests of signals from actual discharges, the peeling of adhesive tapes [6], and the crushing of single crystal quartz and sucrose (known to produce microdischarges in air) showed strong, rapidly rising signals, whereas rapid deformation of polymers showed extremely small signals. Because it is highly likely that the larger signals are due to small bursts of electromagnetic radiation, we refer to them as RE (radiowave emission).

We found that crushing PETN regularly produced large, reproducible RE signals in the coil. The observed electrical signal rose early during the crushing, and frequently consisted of several discrete bursts which are most likely due to individual failure events in the crystal(s). Fig. 3 shows a typical ringing signal (digitized at  $20\ \mu\text{sec}$  per division) due to impact crushing of a single crystal of PETN. The onset of crushing is shown by the arrow. In contrast, crushing RDX did not produce convincing RE signals; thus, we see no evidence of electrostatic discharges during fracture of RDX. This observation is consistent with much lower charge densities on the RDX ejecta in comparison with the PETN ejecta.

### 3.5. Micrographs of ejecta

Morphology and size distribution of ejecta were examined by using optical microscope photographs of the collected particles. The photographs, shown in Figs 4 and 5, represent ejecta caught on microscope

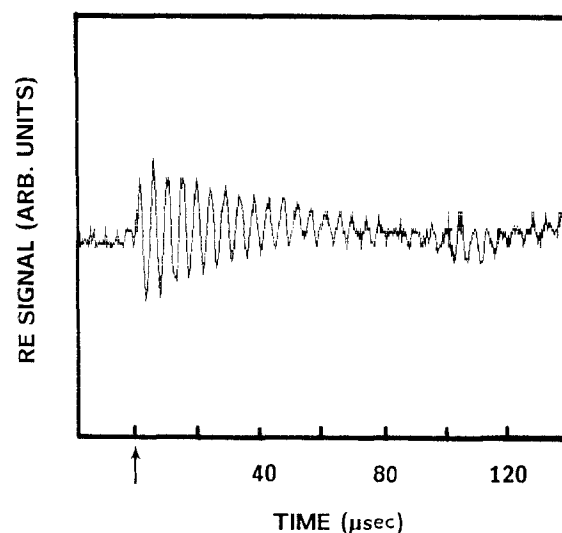


Figure 3 Electrical signal induced in a pick-up coil from crushing PETN.

slides placed near the impact crushing of PETN and RDX. The PETN ejecta (Fig. 4) differ from the RDX ejecta (Fig. 5) in several characteristics. They are more finely divided than RDX ejecta and they always exhibited considerably more clustering. This clustering of PETN ejecta could well be due to the presence of high densities of electrical charge on the fracture surfaces which causes electrostatic attraction agglomeration.

### 3.6. Size distributions

In order to determine a size distribution of the PETN ejecta, we collected several samplings of the ejecta on microscope slides. Using an optical microscope at  $\times 120$ , we counted the number of particles in each size range, employing a geometrically increasing series of sizes [7]. The resulting approximate size distribution is shown in Fig. 6. It shows that most of the collected ejecta are quite small ( $< 5\ \mu\text{m}$ ) and, thus, that the surface area of ejecta will be large, consistent with the findings in our previous fracture-induced ejecta study.

### 3.7. Average charge density

We can combine this particle size distribution with the mass and charge measurements to obtain a value for the average surface charge density on the PETN ejecta. We first assume that the net charge is uniformly distributed over the surface of the particles and that the ejecta are spheres (contrary to what is seen in Fig. 4). This yields a specific surface for these particles of  $2.4 \times 10^5\ \text{mm}^2\ \text{g}^{-1}$ . The ejecta mass collected, typically  $430\ \mu\text{g}$ , and the net charge collected,  $2.5 \times 10^{-10}\ \text{C}$ , results in an average surface charge density of  $2.4 \times 10^{-10}\ \text{C cm}^{-2}$ . The limiting  $E$  field imposed by the occurrence of corona discharge in air [8] is approximately  $2 \times 10^6\ \text{V m}^{-1}$  which will be reached at a surface density of  $1.8 \times 10^{-9}\ \text{C cm}^{-2}$  for uniformly charged spherical particles. An interesting but unanswered question is how does the surface charge vary with size of the PETN ejecta?

We emphasize that these measurements involve only the *net* charge on a large number of particles. The

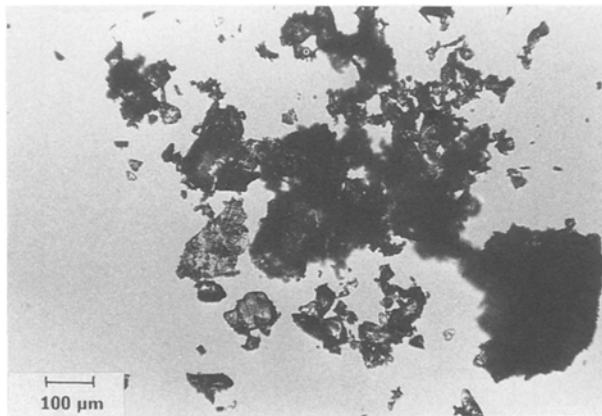


Figure 4 Optical micrograph of PETN ejecta deposited on a microscope slide.

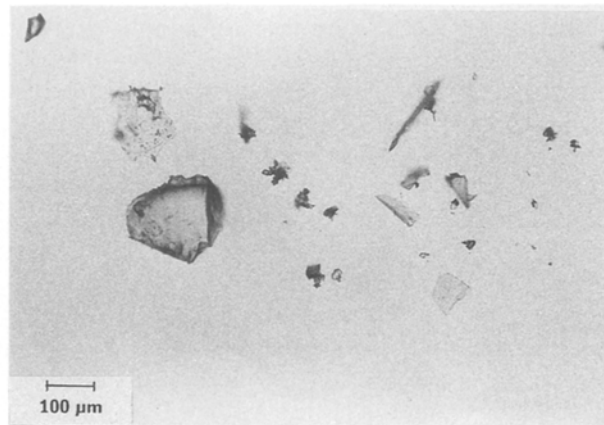


Figure 5 Optical micrograph of ejecta from RDX.

sum of  $\pm Q$ , i.e. the actual charge on the ejecta, could be much greater than the net charge we measure.

There are two possible mechanisms for producing charge on the ejecta by impact loading. First, the crystals undergo a great deal of shear deformation and fracture during crushing. Second, the fragments undergo frictional rubbing by the metal surfaces of the striker and the anvil, both during crushing and subsequently as the ejecta escape. Both of these mechanisms could be contributing to the production of surface charge on the ejecta.

We and other researchers have observed evidence of charge separation accompanying fracture of a number of materials [9–12]. Fracture-induced charge separation is particularly intense in piezo-electric crystals such as  $\text{SiO}_2$  and  $\text{BaTiO}_3$ . PETN has a non-centrosymmetric crystal structure and is known to be piezoelectric whereas RDX and  $\beta$ -HMX (the room-temperature form) are centric and, therefore, non-piezoelectric [11]. This would suggest that ejecta from PETN should carry a greater charge, as is observed, due to charge separation assisted by stress-induced polarization.

Frictional and contact electrification are especially effective in producing charge separation when dissimilar materials, e.g. molecular crystals and metal surfaces, are involved. Thus, we might expect that the crystal fragments would also be charged by rubbing as they glanced off the surfaces during ejection. We cannot rule out this charging mechanism. However, we point out first the striking difference in magnitude of charge on the ejecta from PETN compared with the other two types of explosive crystals, and second, the accompanying RE signals from impact of PETN compared with the lack of RE from RDX. This strongly suggests that the charging of the PETN ejecta is due to deformation and fracture rather than the rubbing that follows.

#### 4. Conclusions

In summary, we have shown the following points.

1. Impact crushing of PETN, RDX, and  $\beta$ -HMX produce large quantities of ejecta.
2. Small ejecta particles had a range in air of at least 6 cm. This would require substantial kinetic energy; however, under the conditions of this experiment the air surrounding the ejecta was put in motion by the

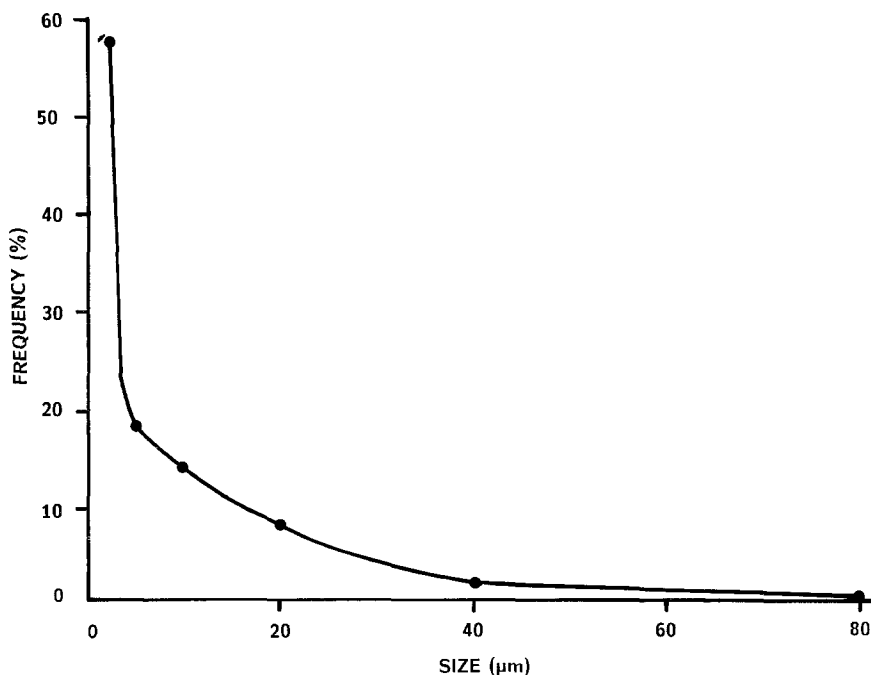


Figure 6 Approximate size distribution of PETN ejecta.

compression of the impact device, thereby entraining the ejecta.

3. The ejecta carry an electrical charge. Their net charge density for PETN approaches the corona limit for surface charge in air. Local charge densities on the ejecta could be greater.

4. The PETN crystals under impact created more finely divided ejecta which was more highly charged than that from RDX and  $\beta$ -HMX crystals. This was demonstrated by measurements of the total charge carried on ejecta, by measurement of the electrical signal produced during crushing and by the subsequent aggregation of the ejecta.

5. We suspect that the charging observed in the case of PETN arises from crushing (fracture) of the crystal rather than collisions with the metal surfaces during ejection.

### Acknowledgements

We thank Dr Howard Cady and Dr Jerry Dick, Los Alamos National Laboratory, for providing the single crystals used in this experiment and Dr Richard Gilardi, Naval Research Laboratory, for helpful discussions. This work was supported by the Office of Naval Research under contract N00014-87-K-0514, Dr R. S. Miller, Program Manager.

### References

1. E. E. DONALDSON, J. T. DICKINSON and S. K. BATTACHARYA, *J. Adhesion* **25** (1988) 281.
2. L. AVRAMI and R. HUTCHISON in "Energetic Materials", Vol. 2, edited by H. D. Fair and R. F. Walker (Plenum, New York, 1977) Ch. 4.
3. C. S. COFFEY and V. R. DeVOST, "Evaluation of Equipment Used to Impact Test Small-Scale Explosive and Propellant Samples" (Naval Surface Weapons Center, Silver Springs, Maryland 1982) NSWC TR 81-215.
4. M. H. MILES, J. T. DICKINSON and L. C. JENSEN, *J. Appl. Phys.* **57** (1985) 5048.
5. E. H. KENNARD, "Kinetic Theory of Gases" (McGraw-Hill, New York, 1983) p. 309.
6. E. E. DONALDSON, X. A. SHEN and J. T. DICKINSON, *J. Adhesion* **19** (1986) 267.
7. T. ALLEN, "Particle Size Measurement" 2nd Edn (Chapman and Hall, London, 1975) Ch. 4.
8. W. R. HARPER, "Contact and Frictional Electrification" (Oxford University Press, London, 1967).
9. J. T. DICKINSON and L. C. JENSEN, *Proc. SPIE Int. Soc. Opt. Engng* **743** (1987) 68, and references therein.
10. J. T. DICKINSON, L. C. JENSEN and A. JAHAN-LATIBARI, *J. Vac. Sci. Technol. A* **2** (1984) 1112.
11. S. G. BOEV and A. N. GALANOV, *Sov. Phys. Solid State* **22** (1980) 1792.
12. J. WOLLBRANDT, V. BRUCKNER and E. LINKE, *Phys. Status Solidi (A)* **77** (1983) 545.
13. H. CADY, Los Alamos National Laboratories, personal communication, 1987.
14. R. GILARDI, Naval Research Laboratories, personal communication, 1987.

*Received 18 April  
and accepted 7 September 1988*